International Journal of Thermophysics, Vol. 27, No. 1, January 2006 (© 2006)
DOI: 10.1007/s10765-006-0031-8

Electrical and Optical Properties of (n)ZnO/(p)CdTe Heterojunction and Its Performance as a Photovoltaic Converter[1]

G. Wary,[2,3] T. Kachary,[4] and A. Rahman[4]

Thin film heterojuctions of the type (n)ZnO/(p)CdTe with different doping concentration were prepared by vacuum evaporation, and their electrical and optical properties, both in dark and under illumination at room temperature as well as elevated temperatures, were studied. Different junction parameters such as ideality factors, barrier heights, Richardson constant, short-circuit current, etc. were determined from I–V characteristics. These parameters were found to change significantly on hydrogenation and annealing of the junctions and also on variation of temperature. The structures showed the change of the photovoltaic (PV) effect, giving a fill factor of 0.57 for hydrogen (H)-treated with an open-circuit voltage of 345 mV and a short-circuit current density of $75.72 \times 10^{-4}\,\mathrm{mA\cdot cm^{-2}}$ and 0.42 for untreated with an open-circuit voltage of 244 mV and a short-circuit current density of $52.00 \times 10^{-4}\,\mathrm{mA\cdot cm^{-2}}$ for doping concentrations of $N_a = 2.43 \times 10^{16}/\mathrm{cm}^3$(2.53% Sb doped CdTe) and $N_d = 3.88 \times 10^{15}/\mathrm{cm}^3$(2.74% Al doped ZnO). The junctions were found to possess a series resistance as high as 437 Ω for an untreated sample and 95 Ω for H-treated samples even under illumination. Proper doping, annealing, and hydrogenation are necessary to reduce the series resistance so as to achieve an ideal solar cell.

KEY WORDS: dangling bond; heterojunction; hydrogenation; PV effect.

[1] Paper presented at the Seventh Asian Thermophysical Properties Conference, August 23–28, 2004, Hefei and Huangshan, Anhui, P. R. China.
[2] Department of Physics, Cotton College, Guwahati-781001, India.
[3] To whom correspondence should be addressed. E-mail: ganesh_wary@yahoo.co.in
[4] Department of Physics, Gauhati University, Guwahati-781014, India.

0195-928X/06/0100-0332/0 © 2006 Springer Science+Business Media, Inc.

1. INTRODUCTION

The investigation of different types of semiconductor heterojunctions for easy photovoltaic solar energy conversion with simple fabrication and low cost has assumed special significance in recent years. As a result, many heterojunction solar cells are currently being explored. A particular class of heterojunction diodes, namely, the oxide semiconductor/semiconductor (base) solar cells have received wide attention [1]. One of them is the ZnO/CdTe anisotype heterojunction. This paper describes recent work on this thin film heterojunction in which one of the semiconductors is (n)ZnO and the other is (p)CdTe. ZnO is a wide bandgap (3.20 eV) II–VI group semiconductor [2]. It is a good candidate for transparent conducting oxides (TCO) and, therefore, can substitute for indium tin oxide (In_2O_3:Sn) and tin oxide (SnO_2) in conductive electrodes of other semiconductor solar cells. Due to its high stability in hydrogen plasma, its nontoxicity, its controllable resistivity, and the low cost of the constituent elements, ZnO has become very attractive for photovoltaic applications [3]. ZnO is widely used in piezoelectric transducers, varistors, gas sensors, and luminescent phosphors [4].

It has also extensive applications in energy efficient windows, liquid crystal displays, optoelectronic devices, etc. On the other hand, CdTe (energy gap = 1.5 eV), a II–VI group intermetallic compound, is a direct bandgap semiconductor. It has a high absorption coefficient which is required for good conversion efficiency. This has led to the investigation of CdTe based heterojunctions and Schottky barrier junctions for use as photovoltaic (PV) devices. The I–V characteristics under illumination of the ZnO/CdTe/Ag junction are reported without a PV efficiency calculation [5]. Sputter deposited (n)ZnO on (p)Zn_3P_2 devices have been reported [6] with PV efficiencies of only 2.0%. A thin film ZnO/p–CdTe photovoltaic device, which showed an efficiency of 3.7%, was reported [7]. One of the more recent applications is the use of ZnO as a substrate for growth of GaN-based materials since the lattice mismatch between GaN and ZnO is relatively small [8].

The origin of the deep levels in ZnO is related to impurities or native defects. The benefits of ZnO include higher resistance to H_2 plasma damage, but studies show that hydrogen atoms can neutralize the excess Zn formed at the surface. Since hydrogen atoms can passivate dangling or defective bonds, the effects of hydrogenation on ZnO material is also very attractive, because its injection produces a significant improvement in the quality of the ZnO crystal. Similarly, hydrogen atoms can neutralize the Cd vacancies and thus, the hydrogen atoms which act as impurities can conversely be separated by the thermal energy [9]. The role of

the hydrogen atom in the CdTe material is also a very attractive area of research because its injection produces a significant improvement in the quality of a CdTe crystal. Furthermore, since the annealing processes are very important in achieving high performance devices, hydrogenation and annealing both play very important roles in enhancing device efficiency.

2. EXPERIMENT

Two thick films of silver, each with a width of 0.5 cm and a length of 2.5 cm, were first deposited by thermal vacuum evaporation on chemically cleaned glass substrates (each of $3 \times 3\,cm^2$ size) at a pressure of 10^{-5} Torr. Above these, a 1.30% Al-doped ZnO film of $(1.5 \times 1.5)\,cm^2$ area was deposited by thermal evaporation from a molybdenum boat. The films were then annealed for 5 h at a temperature of 528 K. Hydrogen gas was then allowed to pass under vacuum conditions for 15 min while maintaining the annealing temperature at 363 K and the pressure at 10^{-4} Torr. Above them, two strips of 1.40% Sb doped CdTe film (each with a width of 0.4 cm and a length of 2.5 cm) were deposited on H-treated (n)ZnO film making crosses with silver strips. The structure was then annealed and treated with hydrogen gas again at 363 K under the same pressure. Finally, two strips of tin (Sn), each with a width of 0.32 cm and a length of 3 cm, were vacuum deposited horizontally over (p)CdTe films for ohmic contacts. Thus, four heterojunctions of equal area ($0.16\,cm^2$) were obtained on the same substrate. Similarly, two other structures of different doping proportions (2.70%Al, ZnO:2.53%Sb, CdTe) and (4.08%Al, ZnO:4.90%Sb, CdTe) were prepared, annealed, and treated with hydrogen. Corresponding unannealed and untreated junction structures were also prepared simultaneously from their respective doping proportions on separate substrates. Thus, a total of six device structures (three for annealed/H-treated and another three for unannealed/untreated having four heterojunctions on each structure) were prepared from three sets of doping proportions while maintaining the same deposition rate. The substrate temperature and pressure were maintained at 350 K and 10^{-5} Torr, respectively, in both cases at the time of film deposition. A schematic diagram of a device structure having four Ag–(n)ZnO/(p)CdTe–Sn junctions is shown in Fig. 1.

For measurements of the conductivity, type, thickness, and spectroscopic analysis, separate substrates were kept under the same conditions and environment as at the time of their respective film deposition. The thicknesses of both (n)ZnO and (p)CdTe were measured outside the vacuum chamber by a multiple beam interference technique, and the thicknesses were verified from the transmittance measurements [10]. For electrical measurements, Ag film deposited on the glass substrate was used as the

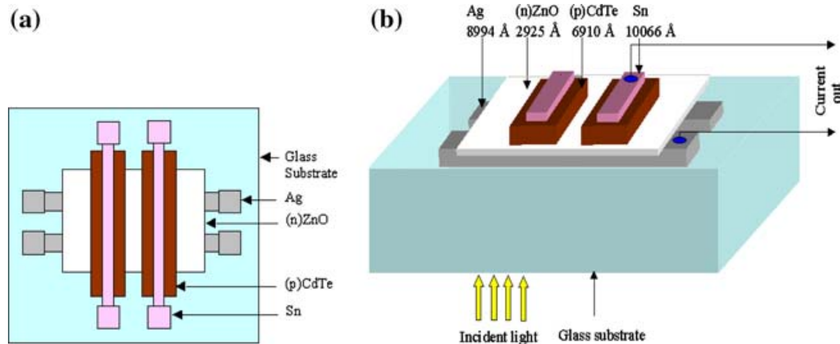

Fig. 1. Schematic diagrams of a Ag–(n)ZnO/(p)CdTe–Sn heterojunction: (a) as prepared (top view) and (b) device structure for electrical connection (not to scale).

lower electrode and Sn film was used as the upper electrode, making the junction structure as Ag–(n)ZnO/(p)CdTe–Sn. The junction, mounted on a specially designed sample holder, was put inside a vacuum chamber for measurement of I–V characteristics under a pressure of 10^{-2} Torr.

The experiment was performed at room temperature as well as at elevated temperature using a specially designed electronic temperature controller. For I–V measurements under illumination, the junction in the chamber was illuminated through a glass window using a white light from a tungsten halogen lamp (500 W). The light radiation was incident from the ZnO side. The input intensity of the light was measured with a lux meter (Luxmat-300ED; Research Ins ND-110028, India) and converted into power (W) by a laser power meter (LPM-20). The type and carrier concentrations were determined by a Hall effect measurement.

3. RESULTS AND DISCUSSION

The contact of the lower electrode Ag (work function = 4.44 eV) [11] with (n)ZnO and the upper electrode Sn (work function 4.43 eV) [11] with (p)CdTe (electron affinity = 4.28 eV) [12] were found ohmic.

The I–V characteristics of (n)ZnO/(p)CdTe junctions in dark and under illumination, respectively, under forward bias both for untreated and hydrogen treated at room temperature (304 K) are shown in Figs. 2 and 3. The junctions exhibited rectifying characteristics both in dark and under illumination. The characteristics under illumination showed a photovoltaic effect and are more rectifying in nature for both H-treated and untreated junctions. However, the characteristics under illumination for H-treated junctions showed a more significant photovoltaic effect than for untreated junctions. Thus, the (n)ZnO/(p)CdTe junction behaves as a junction diode.

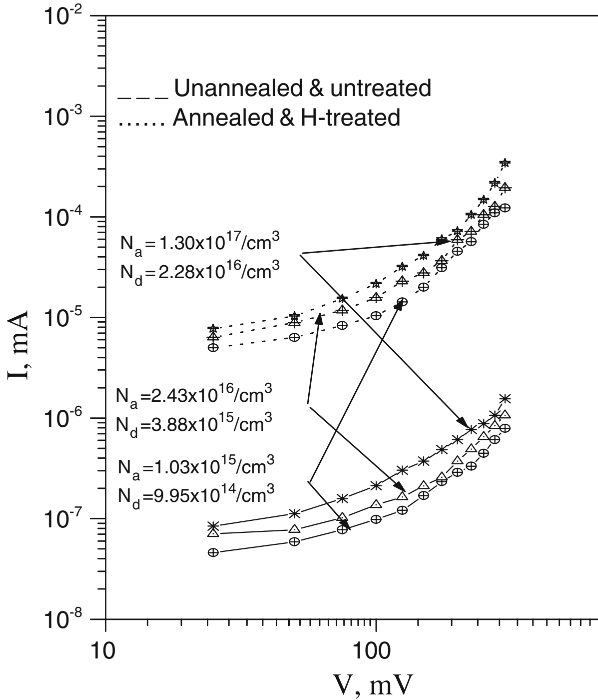

Fig. 2. *I* versus *V* plots at room temperature in dark for different doping concentrations in forward bias (for both H-treated and untreated structures).

Hydrogen was treated to samples keeping the annealing temperature constant at 363 K and the experiment was carried out up to the temperature of 423 K. The passivation effect in In-doped n-CdTe upon exposure of rf hydrogen plasma was studied by electrical (RBA experiment) and photoluminescence (PL) measurements up to 443 K and it was reported that the best passivation occurred at about 423 K [13].

Figure 4 shows the temperature variation of the junction current for several forward bias voltages. With an increase of temperature, the current has been observed to increase, and the slopes at a higher bias voltage are steeper. The current density is given by the expression,

$$J = qA^*TV_{\mathrm{bi}}/k\{\exp(-qV_{\mathrm{bi}}/kT)\}[\exp(qV_{\mathrm{a}}/nT)-1] \quad (1)$$
$$= J_{\mathrm{s}}[\exp(qV_{\mathrm{a}}/nkT)-1]$$
$$\cong J_{\mathrm{s}}[\exp(qV_{\mathrm{a}}/nkT)] \quad (\text{for} V_{\mathrm{a}} \geq 3kT/q) \quad (2)$$

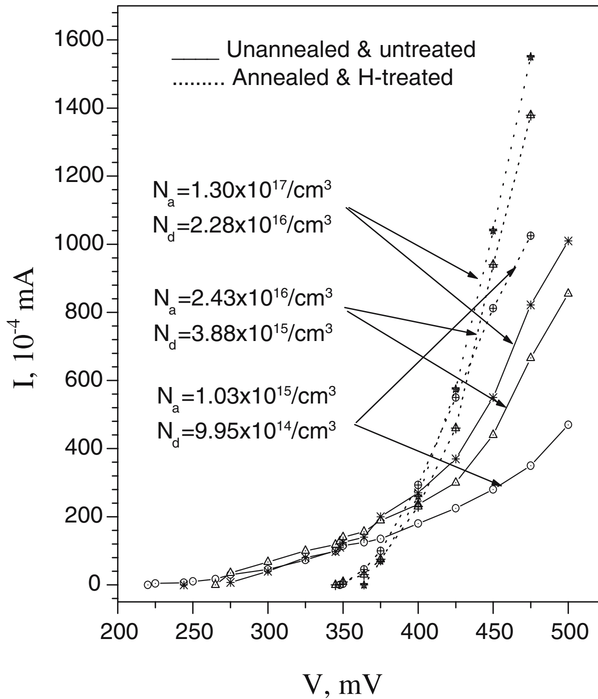

Fig. 3. *I* versus *V* plots at room temperature under illumination for different doping concentrations in forward bias (for both H-treated and untreated structures).

Using Eq. (1), the diode ideality factor '*n*' and reverse saturation current density J_s can be obtained from the $\ln J$ versus V_a plots. Figure 5 shows such plots for a typical junction in dark at room temperature and elevated temperatures. The ideality factor of the junctions studied in the present case was found to vary from 3.81 to 2.08 (untreated) and 3.24 to 1.65 (H-treated) at temperatures from 304 to 423 K satisfying the condition [2],

$$n = q/(kT)[\delta V/\delta(\ln J)] \text{ for} V > 3kT/q \text{ in dark} \tag{3}$$

The presence of an interfacial layer, an image force lowering of built-in potential, a recombination of electrons and holes in the depletion region, and a tunneling effect are the main reasons for the ideality factor to be greater than unity [14]. The reverse saturation current density of a typical junction was found to be 3.32×10^{-10} A·cm^{-2} (untreated) and 3.02×10^{-8} A·cm^{-2} (H-treated) in dark. The same was found to increase with a rise in temperature (Table I). The effective Richardson constant A* and

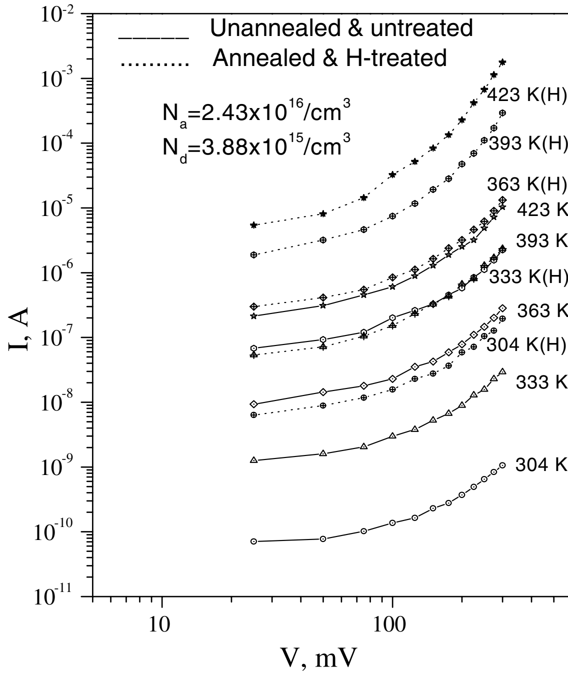

Fig. 4. *I* versus *V* plots for typical junction at different temperatures in dark (for both H-treated and untreated structures).

built-in potential (V_{bi}) of the junctions were calculated from the saturation current density using the relation,

$$J_s = (qA^*TV_{bi}/k)\exp(-qV_{bi}/kT) \quad (4)$$

assuming the built-in potential V_{bi} to be independent of bias. From the $\ln(J_s/T)$ versus T^{-1} plots of a typical junction (Fig. 6), the values of A^* and V_{bi} were found to be 117 $A\cdot cm^{-2}\cdot K^{-2}$ and 0.79 eV, respectively, for H-untreated and 118.5 $A\cdot cm^{-2}\cdot K^{-2}$ and 0.92 eV, respectively, for H-treated structures. The values of A^* and V_{bi} have been observed to increase in H-treated junctions but did not show a significant change with temperature from 304 to 423 K for both cases. There are various factors affecting J–V curves of these junctions. It has been observed that J–V curves are functions of doping concentration and electrode area [15]. In this case, the built-in potential (V_{bi}) plays an important role in the conduction mechanism by the expression,

$$V_{bi} = (kT/q)[\ln(N_a N_d/n_i^2)] \quad (5)$$

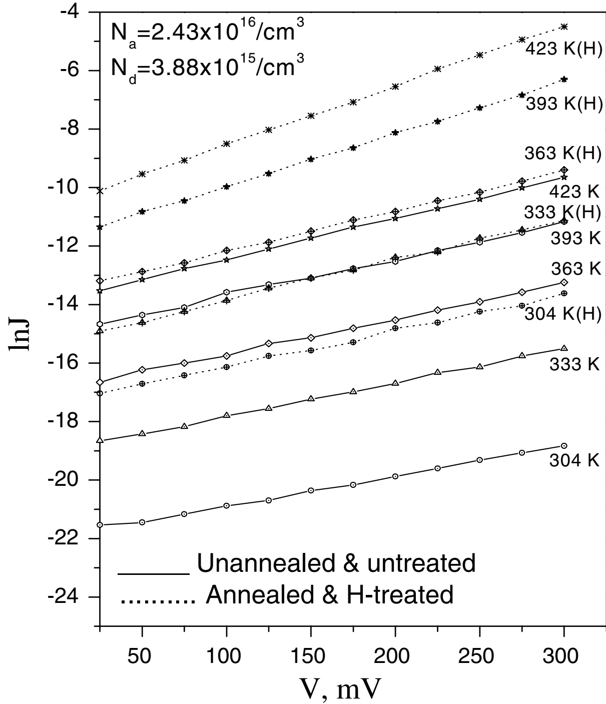

Fig. 5. ln$J$ versus V plots for a typical junction at different temperatures in dark (for both H-treated and untreated structures).

Table I. Variation of Some Parameters of Two Typical Junctions at Different Temperatures in Dark

Temp (K)	J_s(A·cm^{-2})	I.F.(n)	V_{bi}(eV)	A^*(A·cm^{-2}·K^{-2})
(a) Untreated structure (Sample No. 25w$_1$)				
304	3.32×10^{-10}	3.81		
333	5.56×10^{-9}	2.98		
363	4.38×10^{-8}	2.59	0.79	117
393	2.84×10^{-7}	2.27		
423	1.18×10^{-6}	2.08		
(b) H-treated structure (Sample No. 25w$_2$)				
303	3.02×10^{-8}	3.24		
333	2.75×10^{-7}	2.41		
363	1.51×10^{-6}	2.18	0.92	118.5
393	7.55×10^{-5}	1.58		
423	2.76×10^{-5}	1.65		

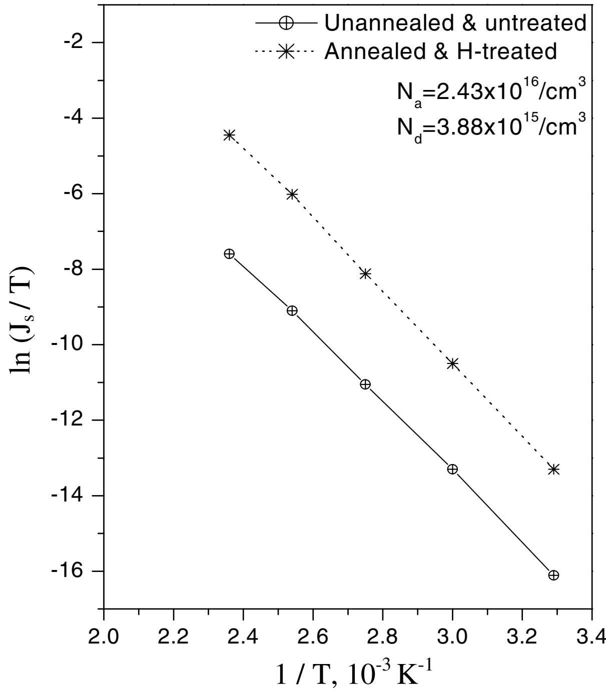

Fig. 6. $\ln(J_s/T)$ versus $1/T$ plots.

where n_i is the intrinsic carrier concentration, N_a is the acceptor concentration, and N_d is the donor concentration. Thus, it is clear from Eqs. (4) and (5) that the saturation current density increases (conductivity increases) with an increase of V_{bi} due to an increase of doping concentrations N_a and N_d (an exponential decrease of V_{bi} is dominated by an exponential increase of the applied voltage V_a).

The junctions were studied for their PV performance. The structures exhibited a PV effect characterized by a high series resistance in their I–V characteristics (Fig. 7). The open-circuit voltage (V_{oc}) of different junctions were found to increase from 220 to 265 mV and the short-circuit current (I_s) from 51.04×10^{-7} to 56.00×10^{-7} A·cm^{-2} with a fill factor from 0.39 to 0.45 for untreated junctions; and the corresponding variations for H-treated junctions are 348 to 364 mV, $74.00 \times l0^{-7}$ to 76.30×10^{-7} A·cm^2, and 0.56 to 0.58, respectively (Table II). The results follow the well known expressions,

$$I_{sc} = I_s[\exp\{q(V\text{-}IR_s)/kT\} - 1] - I \quad (6)$$

$$V_{oc} = (nkT/q)\ln[(I_{sc}/I_s) + 1] \quad (7)$$

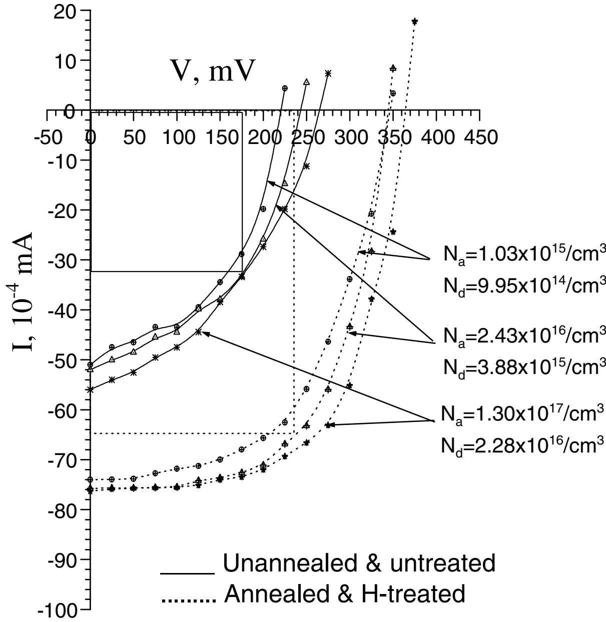

Fig. 7. *V* versus *I* (reversed current) plots under illumination for H-treated and untreated structures at room temperature.

where I is the total output current, R_S is the series résistance, and I_S is the diode saturation current. The series resistance (which causes the short circuit current) is responsible for increasing the V_{oc} value; as at room temperature, the diode saturation current is constant. Another important factor studied in the structure was the presence of a high series resistance (R_S) associated with the neutral regions of the semiconductor layers of (n)ZnO and (p)CdTe. The series resistance of a heterojunction depends upon the junction depth, impurity concentrations of p-type and n-type regions, and the arrangement of the front surface ohmic contact. It is found in a depth profile study of (p)CdTe that carrier concentrations of hydrogenated and annealed films increase with depth [9]. So the resistivity of the (p)CdTe decreases towards the junction but not to the top surface of the (p)CdTe film in the present arrangement.

Another reason is the increase of the diffusion coefficient due to hydrogenation which can be described by the following expression [16],

$$D_{\mathrm{H}} = D_{\mathrm{O}} \exp(-E_{\mathrm{a}}/\mathrm{k}T) \qquad (8)$$

Table II. Variation of Some Parameters of Three Different Junctions under Illumination at Room Temperature (for both H-treated and untreated samples)

Doping concentration		Unannealed & untreated				Annealed & H-treated			
$N_a(\text{cm}^{-3})$	$N_d(\text{cm}^{-3})$	Sample No	$I_{sc}(10^{-4}\,\text{mA})$	V_{oc} (mV)	FF(%)	Sample No	$I_{sc}(10^{-4}\,\text{mA})$	V_{oc}(mV)	FF (%)
1.03×10^{15}	9.95×10^{14}	$24w_1$	51.04	220	39.37	$24w_2$	74.00	348	56.48
2.43×10^{16}	3.88×10^{15}	$25w_1$	52.00	244	41.69	$25w_2$	75.72	345	56.82
1.30×10^{17}	2.28×10^{16}	$26w_1$	56.00	265	45.42	$26w_2$	76.30	364	57.51

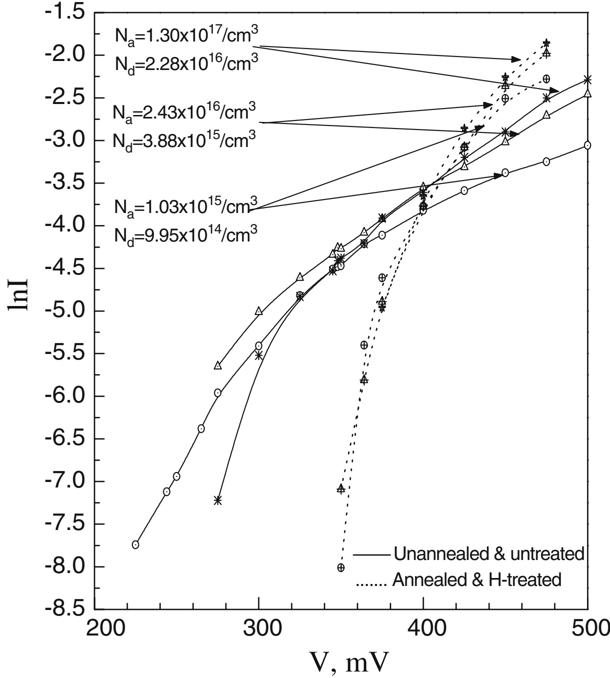

Fig. 8. ln$I$ versus V plots to determine deviation ΔV from linearity at different currents.

where D_O is the diffusion coefficient for an untreated sample, E_a is the activation energy of the hydrogen diffusion, k is Boltzmann's constant, and T is the absolute temperature. The enhancement of the hydrogen motion, therefore, indicates the decrease in the activation energy E_a and increase in the conductivity as given by the expression [17],

$$\sigma_H = (4\pi m^* kTq^2 d/h^3)[\exp(-E_a/kT)] \quad (9)$$

where the first term within the brackets along with the effective mass (m^*) and the grain size (d) are constant. Thus, the resistance decreases after annealing in hydrogen. An estimate of the series resistance was carried out for the forward bias from V versus ln$I$ plots (Fig. 8) and then from ΔV versus I plots (Fig. 9) where ΔV in the deviation from linearity along the voltage scale for a fixed current. For two typical junctions (one for unannealed/untreated and other for annealed/H-treated), results show that the devices possess a series resistance as high as 437 Ω (untreated) and 91 Ω (H-treated) under illumination. In both cases, R_s

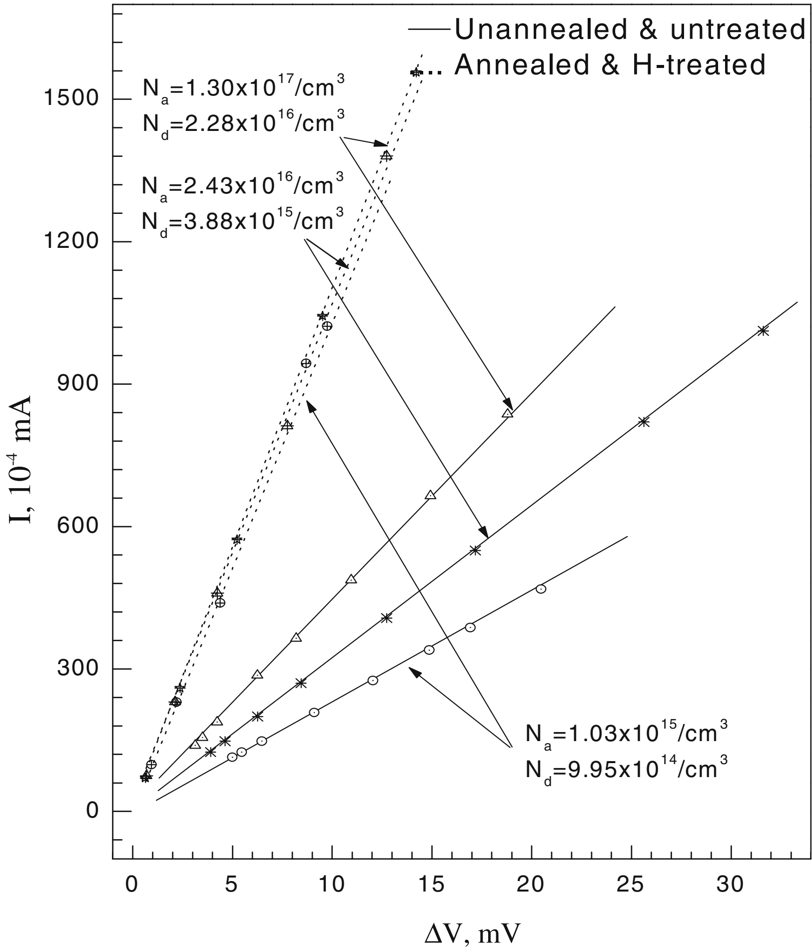

Fig. 9. *I* versus ΔV plots to determine series resistance of the junctions.

has been found to decrease with increasing doping concentration but the lower value of the series resistance observed in an annealed/H-treated sample rather than an untreated sample is mainly the result of the combined effect of an increase in the diffusion coefficient and an increase in the conductivity due to hydrogenation. So a decrease of the series resistance increases the short circuit current as well as the open circuit voltage. The observed deviation from exponential behavior at a voltage higher than 500 mV (not shown here) was due to the limitation of the current by the high series resistance of the junction [18].

At a large forward current, the voltage drop across the series resistance causes the actual voltage drop across the barrier region to be less than the voltage applied to the terminals of the junction. Thus, I-V curves deviate from the ideal condition and the current is proportional to $\exp[q(V - IR_S)/kT]$.

4. CONCLUSION

Junction parameters such as the barrier height, the diode ideality factor, and the Richardson constant of a vacuum deposited (n)ZnO–(p)CdTe structure were determined from its I–V characteristics. They are found to change under illumination and with a change in temperature. The junction, though rectifying, is characterized by a high series resistance. Proper doping, annealing, and hydrogenation are necessary to reduce the series resistance in order to achieve a high performance solar cell. Further studies are in progress in this direction.

REFERENCES

1. V. K. Jain, in *Physics of Solar Cells*, First Ed., S. C. Jain, S. Radhakrishna, and T. R. S. Reddy, eds. (International Council of Scientific Unions, Madras, India, 1984), p. 111.
2. S. M. Sze, in *Physics of Semiconductor Devices*, 2nd Ed. (Wiley Eastern limited, New Delhi, reprint, 1983), p. 291.
3. B. Joseph, K. G. Gopchandran, P. K. Manoj, P. Koshy, and V. K. Vaidyan, *Bull. Mater. Sci.* **22:**921 (1999).
4. M. Rebien, W. Henrion, M. Bär, and Ch.-H. Fischer, *Appl. Phys. Lett.* **80:**3518 (2002).
5. B. R. Mehta, S. Kumar, K. Singh, and K. L. Chopra, *Thin Solid Films* **164:**265 (1988).
6. K. W. Mitchell, in *Physics of Solar Cells*, First Ed., S. C. Jain, S. Radhakrishna, and T. R. S. Reddy, eds. (International Council of Scientific Unions, Madras, India, 1984), p. 159.
7. M. S. Tomar, *Thin Solid Films* **164:**295 (1988).
8. S. K. Nandi, S. Chatterjee, S. K. Samanta, G. K. Dalapati, P. K. Bose, S. Varma, S. Patil, and C. K. Maiti, *Bull. Mater. Sci.* **4:**365 (2003).
9. M. D. Kim, T. W. Kang, and T. W. Kim, *Appl. Surface Sci.* **137:**57 (1999).
10. G. Wary and A. Rahman, *Proc. Sixth Asian Thermophys. Props. Conf.*, M. N. Bora, ed., ATPC 2001, Guwahati, India (2001), Vol. II, p. 579.
11. E. H. Rhoderick, *Metal-Semiconductor Contacts* (Clarendon Press, Oxford, Scotland, 1978), p. 54.
12. R. K. Swank, *Phy. Rev.* **153:**844 (1967).
13. S. Gurumurthy, H. L. Bhat, B. Sundersheshu, R. K. Bagai, and V. Kumar, *Appl. Phys. Lett.* **68**:2424 (1996).
14. H. K. Henisch, *Semiconductor Contacts* (Clarendon Press, Oxford, New York, 1984), p. 23.

15. P. C. Sarmah and A. Rahman, *Bull. Mater. Sci*. **24:**411 (2001).
16. R. Singh and S. Prakash, *Pramana-J. Phys*. **61:**121 (2003).
17. S. N. Singh, B. K. Das, R. C. Narula, and S. C. Jain, in *Photovoltaic Materials and Devices*, B. K. Das and S. N. Singh, eds. (Wiley Eastern Limited, New Delhi, 1984), p. 99.
18. I. Günall and M. E. Özsan, *Thin Solid Films* **113:**189 (1984).